RPE | Radiation Physics & Engineering
An International Peer-Reviewed Journal
Published by K.N. Toosi University of Technology
http://rpe.kntu.ac.ir
Research Article

Radiation Physics and Engineering 2022; ?(?):?–?
https://doi.org/

Effects of fusion plasma ions on Aluminum and Tungsten samples using a plasma focus device: a comparison study

Ali Adeli Ahmadabadi, Zahra Shahbazi rad*, Fereydoun Abbasi Davani, Behjat Ghasemi
Radiation Application Department, Faculty of Nuclear Engineering, Shahid Beheshti University, Tehran, Iran

HIGHLIGHTS

- The plasma ions -fusion material interaction was investigated.
- The effect of plasma ions on Aluminum and Tungsten as fusion reactor material was investigated.
- The sample analyses were done by the SEM, EDX, ERD and RBS methods.

ABSTRACT

In this research, the effect of ions produced in deuterium plasma on Tungsten (W) and Aluminum (Al) plates has been investigated using a plasma focus device with the specifications of (C=10.4 μF, V=23 kV, E=2.75 kJ). The W samples used because it is one of the key elements in the Tokamak device. Because we wanted to put the W samples at the distance from the anode top with maximum plasma produced ions, we should find the optimum place. Due to the high cost of W samples, we used Al samples to find the optimal conditions. The samples were irradiated at 8 cm distance from the anode top with deuterium ions produced by a plasma focus device. The sample analyses were done by the SEM and EDX methods. The sample irradiation by deuterium plasma ions caused a lot of damages and bubble formation on the sample surfaces. The analyses showed the extent of surface damage and the number of ions deposited on the surface. The number of damages on the Al surface was much higher than W. Bubbles were formed on the surface were due to the impact of deuterium ions on the W and Al samples. Also, the deuterium ion energy was measured with a Faraday cup as about 50 keV.

KEYWORDS
Plasma focus
Deuterium plasma ions
W
Al
Faraday cup

HISTORY
Received: ?
Revised: ?
Accepted: ?
Published: ?

1 Introduction

Due to the human need for energy and also the shortage of fossil fuels in the near future, it is necessary to replace energy resources, one of which is the nuclear fusion. Because of the advantages and unlimited fuel materials, scientists are looking for exploiting fusion energy. The Tokamak is a device (i.e, fusion reactor) designed for exploiting fusion energy. With the walls made of beryllium (Be) and Tungsten (W) (Philipps, 2011). The Joint European Torus (JET) is the largest present-day Tokamak, i.e. a magnetic controlled thermonuclear fusion device for energy research (Rubel et al., 2008). To achieve further progress in controlled fusion, the ITER-Like Wall (ILW) Project at JET is underway in order to explore Tokamak metal wall: Be in the main operation and plasma-wall interaction processes with a full chamber and W in the divertor (Rubel et al., 2008). In their project, Rubel et al (Rubel et al., 2008) irradiated Be under radiation fusion radiation for 10 s. Therefore, using a thermal generator, the effects of plasma inside Tokamak on W and Be were simulated and investigated.

A plasma focus (PF) device is one of the most widely used devices for thermonuclear fusion researches. The plasma focus device was invented separately in the early 1960s by Mather (Mather, 1965) in the United States and Filippov (Filippov, 1962) in the Soviet Union. The plasma dynamics and formation of ion plasma in PF device was reported elsewhere (Rawat, 2015). Pimenov et al. (Pimenov et al., 2008) tested W and Al with deuterium plasma irradiated by a PF-1000 device, where the target materials were placed at a distance of 30 cm from the anode. They observed microcracks in W formation and bubbles in Shirokova et al. (Shirokova et al., 2013) irradiated as samples, W and W doped with 1% lanthanum-oxide La_2O_3 (WL10) samples with deuterium plasma ions ions at the of 6.5 cm

*Corresponding author: z_shahbazi@sbu.ac.ir

from the anode of a PF-12 device, these were placed at a distance of 6.5 cm from the anode. They concluded that the length of macroscopic damages is bigger for WL10 than for pure Javadi et al. (Javadi et al., 2018) Investigated the effects of hot dense decaying pinch plasma, highly energetic deuterium ions and fusion neutrons generated in a low-energy (3.0 kJ) plasma focus device on the structure, morphology and hardness of the W samples surfaces. W samples were irradiated using various distances from the top of the anode (5, 7, 9 and 11 cm) using a fixed number (5) of plasma focus shots. The sample exposed at 7 cm showed more drastic changes compared to that of the sample exposed at a closer distance of 5 cm. They concluded that the proximity of the sample exposed at 5 cm resulted in the generation of intense backward-moving secondary-plasma from the sample surface due to fast plasma stream impact, which significantly interferes with an ongoing pinch. However, at larger distances, 9 and 11 cm, of exposure, the surface structural damage was reduced due to a decrease in energy and number flux of high-energy ions and hot plasma stream due to their diverging nature. There are more researches in the following references (Demina et al., 2009; Shirokova et al., 2014; Cicuttin et al., 2015; Väli et al., 2016; Quirós et al., 2017; Linsmeier et al., 2017; Seyyedhabashy et al., 2020; Vas et al., 2021; Raeisdana et al., 2020).

In the Tokamak device the deutrium gas is used to create fusion. When the produced Deutrium plasma interacts by the device wall, the wall material might be harmed. So, the wall material should have the highest strength. Many researches are still being done to improve the fusion process, in this context, using a plasma focus device called SBUPF1, the effect of deuterium plasma on a W sample has been investigated and compared with the effect of deuterium plasma on an Al sample.

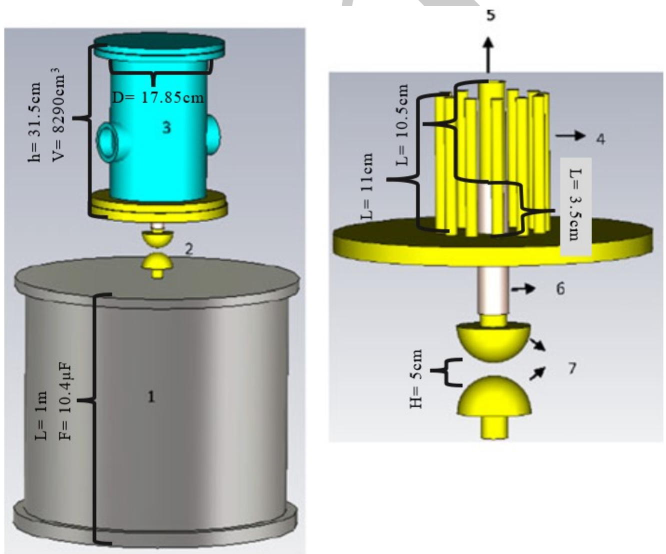

Figure 1: SBUPF1 schematic diagram, 1) capacitor, 2) and 7 trigatron spark gap, 3) PF chamber, 4) cathodes, 5) anode, 6) insulator sleeve (Shahbazi rad et al., 2011).

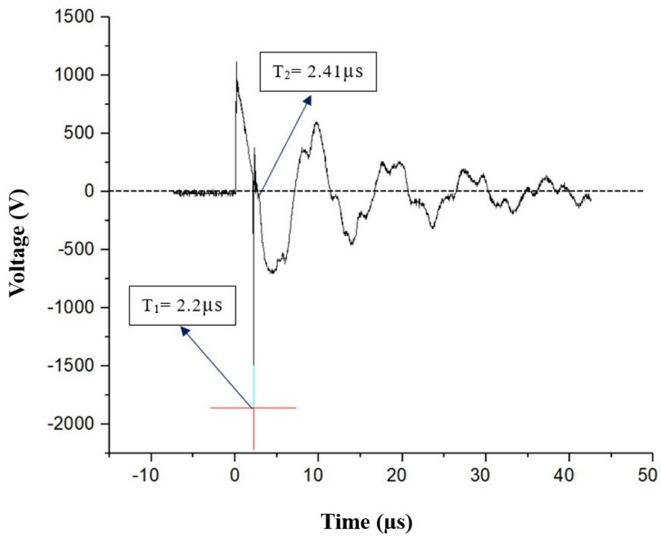

Figure 2: The $\frac{\mathrm{d}I}{\mathrm{d}t}$ signal shows pinch formation time at a pressure of 6 mbar and a charging voltage of 23 kV (T_1 is a pinch time and T_2 is the time when voltage is 0).

2 Experimental Setup

The measurements were performed using the low-energy Mather-type plasma focus device SBUPF1 with a maximum supplied energy of 2.75 kJ.

A schematic diagram of the SBUPF1 device is shown in Fig. 1 (Shahbazi rad et al., 2011). The device contains a copper rod (anode) with the diameter of 2.2 cm and the height of 12 cm as well as twelve copper rods (cathods) with a diameter of 1 cm and a height of 11 cm. The anode is separated from the steel housing by an insulator (Pyrex Glass). The chamber was made of steel with the diameter of about 18 cm, its height is about 31.5 cm and the volume of the chamber is about 8300 cm^3. The chamber was evacuated to a pressure of 2×10^{-2} mbar using a rotary pump. The amount of vacuum is sufficient for the measurements. However, the higher the vacuum level, the fewer impurities are in the sample and as a result more accurate measurements are expected. The anode is connected to the capacitor bank by a switch (air gap switch). The device is powered by a capacitor of 10.4 μF and maximum voltage storage of up to 23 kV (Shirani and Abbasi, 2010).

In these measurements, the maximum discharge current, as well as the optimal plasma conditions, were measured using a Rogowski coil and Oscilloscope (Pokryvailo and Kushnerov, 2006). Depending on the geometry of the Rogowski coil, the signal derived from the discharge current is formed. By considering this signal, both the maximum discharge current and the optimal working conditions for different gases can be obtained.

First, for each working gases, the optimum voltage and pressure were determined to obtain the best discharges for maximum ion density. For this reason, at each voltage and pressure, the derived current of the system which is measured with the Rogowski coil was recorded. The time interval between the operating time pinches and the

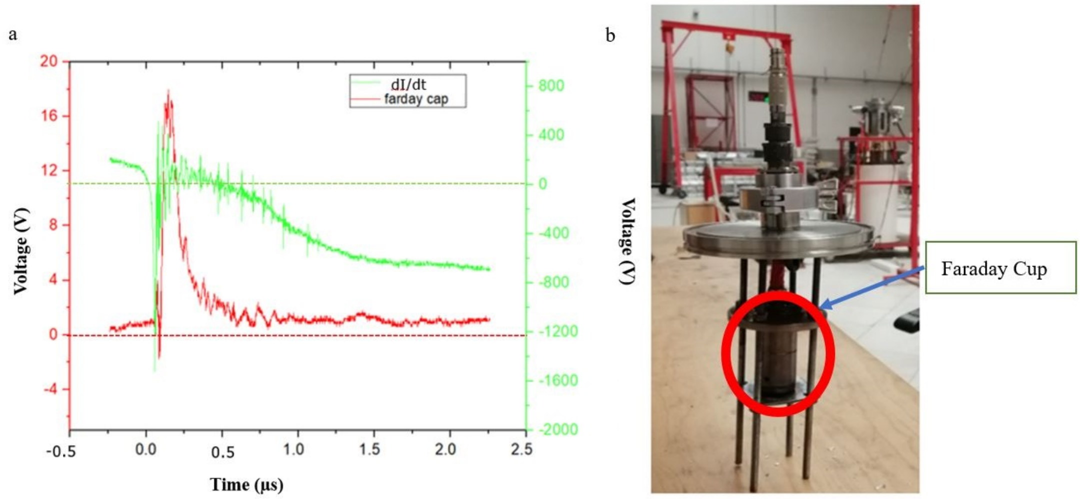

Figure 3: a) Signals after the creation of deuterium plasma at a pressure of 6 mbar and a voltage of 23 kV. The red signal represents the Faraday Cup signal and the green signal represents $\frac{\mathrm{d}I}{\mathrm{d}t}$, b) the holder for samples and Faraday Cup.

time of maximum current was the criterion for finding the optimum operating time. The smaller value of this criterion meant that the pinch occurred at the time near the maximum current or derived resulted high ion emission (Shahbazi rad et al., 2011).

Due to the inductive properties of the plasma focus device, the discharge of the current is a damped sinusoidal wave. The Rogowski coil records a signal that is proportional to the discharge induced current. At the moment of pinch, the resistance of the plasma focus device increases but the current decreases. The closer pinch time is to the maximum time of discharge of the current, the maximum energy of the capacitor is transferred to the pinch column and then a stronger pinch is created. The time interval between the gap created in the current signal and the time of zero current derivative is an appropriate criterion for comparing the plasma pinch power in different discharges. To investigate the effect of deuterium plasma on W and Al surfaces, the optimum pressure and charging voltage for deuterium gas was primarily obtained. By examining different pressures and voltages, the optimal pressure and charging voltage values for deuterium gas were obtained as 6 mbar and 23 kV, respectively. Figure 2 shows the current derivative signal and the fitted curve for a discharge of a plasma focus device at the pressure of 6 mbar of deuterium gas and the voltage of 23 kV.

Also, a Faraday Cup was used to calculate the ion energy. The time of flight (TOF) method was for ion energy measurement. The time difference between the pinch creation and the time of the maximum ion count of the Faraday Cup signal is measured as TOF. TOF of ions devided by the distance from the anode top equals the maximum ions velocity (v). Also, the energy spectrum of deuterium ions was obtained by the classical kinetic energy formula ($k = \frac{1}{2}mv^2$). Figure 3-a shows $\frac{\mathrm{d}I}{\mathrm{d}t}$ and the signals of Faraday Cup used for the TOF can be measured. Figure 3-b shows the Faraday Cup in its holder where the outer shell and inner cup were made of brass and a layer of graphite was added to the inner cup. Faraday Cup has an aperture of 500 μm with an insulation made of polyethylene.

The Al and W samples with the 3 cm length, 3 cm width and 1 mm thickness were placed at the center of the plasma focus device on the anode top with the holder shown in Fig. 3-b. The samples were placed at 8 cm distance from the ande top. Each sample was irradiated with 3 shots.

The surface of the samples was cleaned with methanol alcohol before measurements since the interaction of produced ions with the sample surface increases the temperature of the sample, the heat treatment is not required.

After irradiating with deuterium plasma ions, the samples were analyzed with SEM (Scanning Electron Microscope) and EDX (Energy Dispersive X-Ray) methods (Pokryvailo and Kushnerov, 2006; Eaglabs, 2009; Bird and Williams, 1989; Chu et al., 1978; Kakuee et al., 2012; Tesmer and Nastasi, 1995) and (http://mee-inc.com/eds.html). The SEM and EDX analyses were done by SEM microscope (SU3500) at the Central Laboratory of Shahid Beheshti University.

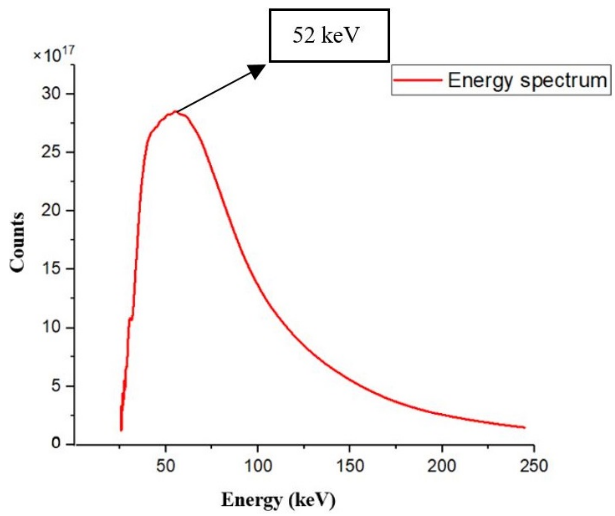

Figure 4: The energy distribution of deuterium ions.

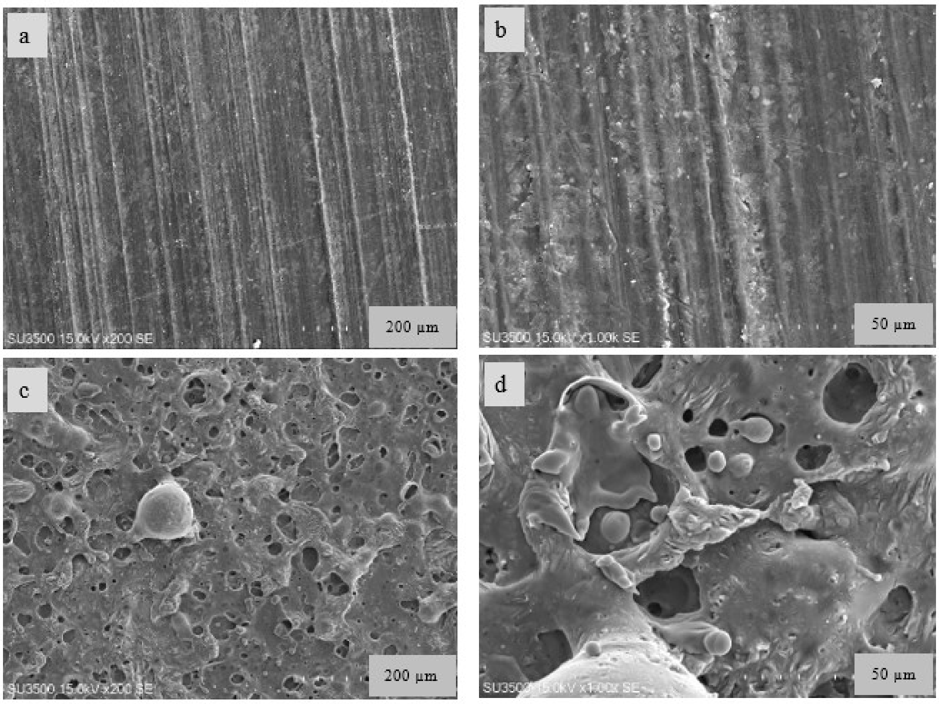

Figure 5: Al sample SEM image ('a' and 'b') before ('c' and 'd') after irradiation by deuterium plasma ions at the pressure of 6 mbar and the voltage of 23 kV with different magnifications.

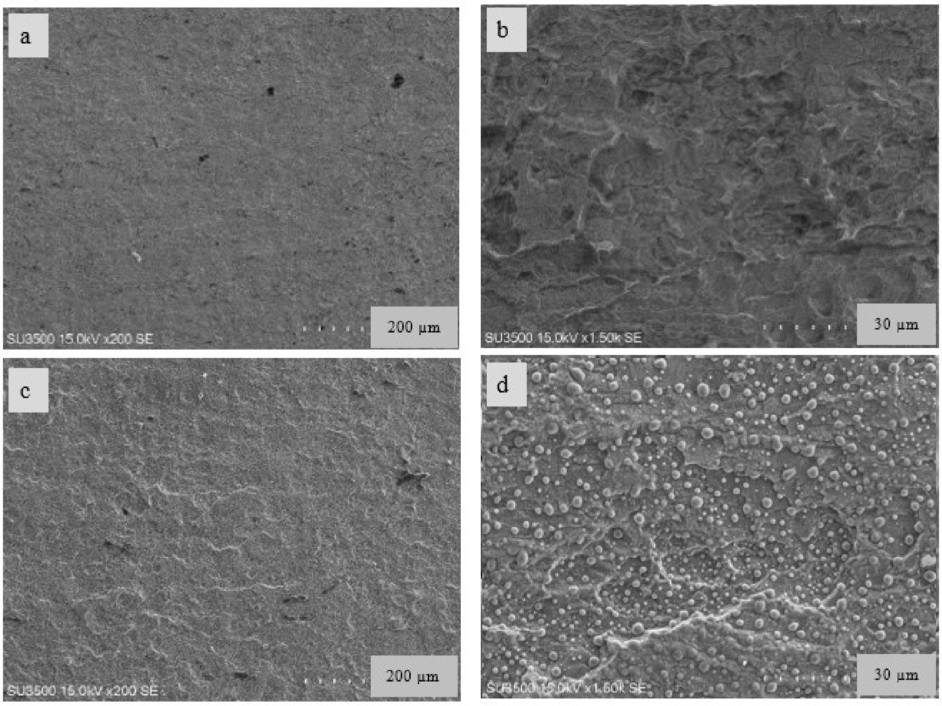

Figure 6: W sample SEM image ('a' and 'b') before ('c' and 'd') after irradiation by deuterium plasma ions at the pressure of 6 mbar and the voltage of 23 kV with different magnifications.

3 Results and Discussion

According to the signals recorded by the Rogowski coil, the optimal conditions for deuterium gas were 6 mbar and 23 kV for gas pressure and charging voltage, respectively. The maximum discharge current was measured at 110 kA. The Faraday Cup was placed at a distance of 14 cm from the anode top. The energy spectrum distribution of deuterium ions was obtained with TOF methods as shown in Fig. 4. The maximum deuterium ion energy was measured as about 52 ± 7.2 keV. Al and W samples were analyzed before and after deuterium plasma irradiation. The SEM images of the surface of the Al sample before and after deuterium plasma irradiation can be observed

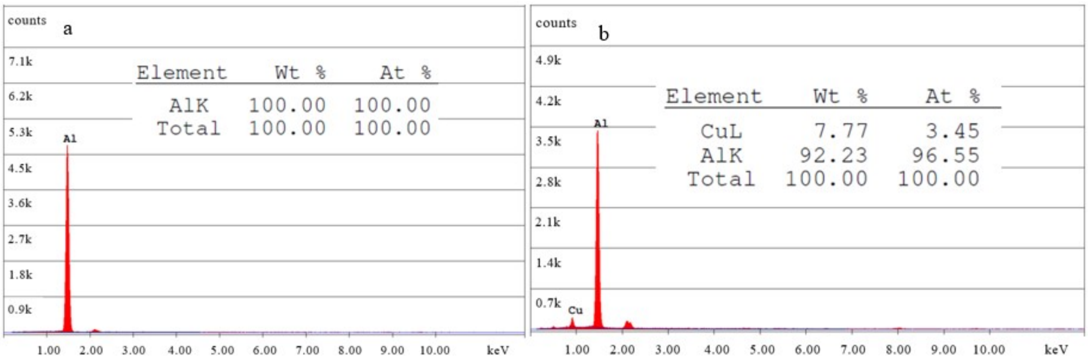

Figure 7: The EDX analysis of Al sample (a) before (b) after irradiation by deuterium plasma ions at the pressure of 6 mbar and the voltage of 23 kV.

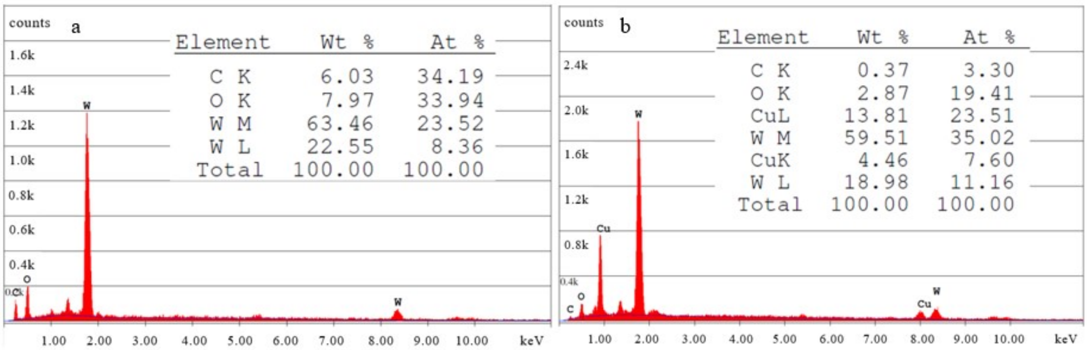

Figure 8: The EDX spectroscopy W sample (a) before (b) after irradiation with deuterium plasma at a pressure of 6 mbar and a voltage of 23 kV.

in Fig. 5. Due to deuterium plasma irradiation, lot of damages were observed and bubbles were formed on the surface. The SEM images of the W sample surface before and after deuterium plasma irradiation, are shown in Fig. 6. Deuterium plasma irradiation did not cause much damage to the W surface, whilst bubbles were still formed on the surface. According to the SEM analysis of W and Al surfaces irradiated by deuterium plasma ions, the number of bubbles in the Al surface was less and the bubble radius was larger than the W sample and also the larger surface degradation of the Al sample was observed. These results may be due to the lower resistance of Al compared to W.

The EDX spectroscopy of the samples was carried out to investigate the sample both quantitively and qualitatively. The results of EDX spectroscopy of Al samples are shown in Fig. 7. The EDX spectroscopy of the unexposed sample (Fig. 7-a) shows that the only element in the sample is Al. The EDX analysis of the deuterium ion-exposed Al sample demonstrates that Al and Cu (Copper) exist in the sample. The elemental analysis (Fig. 7-b) shows that the percentage of Al and Cu are 92.23% and 7.77%, respectively. This analysis may be considered as evidence that after the exposure, some penetration of Cu into the samples is occurred. Note that the anode is made of Cu, and the sputtering of Cu due to electron strike on the top of the anode takes place during PF pinch.

The results of EDX spectroscopy of W samples are shown in Fig. 8. The EDX analysis of the unexposed sample (Fig. 8-a) shows that the elements exist in the sample are W, O (Oxygen), and C (Carbon) with percentages of 86%, 7.97%, and 6.03%, respectively. The EDX analysis of the deuterium ion-exposed W sample shows that Al and Cu exist in the sample. The elemental analysis (Fig. 8-b) shows that the percentages of W, O, and C are 78.49%, 18.27%, and 0.37%, respectively.

4 Conclusions

Due to the importance of the effect of plasma-produced species on the materials in fusion reactors, the effects of deuterium plasma ions on Al and W were investigated using a plasma focus device. The following results were obtained in these measurements. According to Figs. 5 and 6, after irradiating Al and W samples with deuterium plasma ions, lots of damages and bubbles were created on the sample surface. It was observed that the number of bubbles on the Al surface was less and the size of the bubble radius was higher than the one in W. Also, the surface degradation of the Al sample was more than that of W. According to Figs. 7 and 8, the reason for the presence of Cu on the samples is the presence of a Cu cathode and anode and the sputtering of Cu from their surface in the process of plasma formation. Also, the oxygen in the samples may be due to impurities in the produced plasma due to an insufficient initial vacuum and may also be emitted from the copper anode as impurities.

References

Bird, R. C. and Williams, J. S. (1989). *Ion beams for materials analysis*. Elsevier.

Chu, W.-K., Mayer, J., and Nicolet, M.-A. (1978). Backscattering Spectrometry Academic Press. *New York*.

Cicuttin, A., Crespo, M., Gribkov, V., et al. (2015). Experimental results on the irradiation of nuclear fusion relevant materials at the dense plasma focus Bora device. *Nuclear Fusion*, 55(6):063037.

Demina, E., Dubrovsky, A., Gribkov, V., et al. (2009). Application of a plasma accelerator of the dense plasma focus type in simulation of radiation damage and testing of materials for nuclear systems. In *International Topical Meeting on Nuclear Research Applications and Utilization of Accelerators, IAEA, Vienna*.

Eaglabs (2009). Scanning Electron Miceoscopy (SEM)/ Energy Dispersive X-ray Spectroscopy (EDS) Services. *Technique Note*.

Filippov, N. (1962). Plasma Focus Studies in Serbia. *Nuclear Fusion, Suppl., Part*, 2:557.

Javadi, S., Ouyang, B., Zhang, Z., et al. (2018). Effects of fusion relevant transient energetic radiation, plasma and thermal load on PLANSEE double forged tungsten samples in a low-energy plasma focus device. *Applied Surface Science*, 443:311–320.

Kakuee, O., Fathollahi, V., Lamehi-Rachti, M., et al. (2012). Ion beam analysis of hydrogen-treated Ti/TiN protective nanomultilayers. *Acta Physica Polonica, A.*, 122(1).

Linsmeier, C., Unterberg, B., Coenen, J., et al. (2017). Material testing facilities and programs for plasma-facing component testing. *Nuclear Fusion*, 57(9):092012.

Mather, J. W. (1965). Formation of a high-density deuterium plasma focus. *The Physics of Fluids*, 8(2):366–377.

Philipps, V. (2011). Tungsten as material for plasma-facing components in fusion devices. *Journal of Nuclear Materials*, 415(1):S2–S9.

Pimenov, V. N., Demina, E. V., Ivanov, L., et al. (2008). Damage and modification of materials produced by pulsed ion and plasma streams in dense plasma focus device. *Nukleonika*, 53:111–121.

Pokryvailo, A. and Kushnerov, A. (2006). Design of Design of Rogowski Rogowski coil with integrator. *Project on course at Ben-Gurion University, Negev*.

Quirós, C., Mougenot, J., Lombardi, G., et al. (2017). Blister formation and hydrogen retention in aluminium and beryllium: A modeling and experimental approach. *Nuclear Materials and Energy*, 12:1178–1183.

Raeisdana, A., Kiai, S., Sadighzadeh, A., et al. (2020). Measurement of Ion Energy by TOF Detection Technique in a Dense Plasma Focus Device. *Journal of Fusion Energy*, 39(5):292–296.

Rawat, R. (2015). Dense plasma focus-from alternative fusion source to versatile high energy density plasma source for plasma nanotechnology. In *Journal of Physics: Conference Series*, volume 591, page 012021. IOP Publishing.

Rubel, M. J., Bailescu, V., Coad, J., et al. (2008). Beryllium plasma-facing components for the ITER-like wall project at JET. In *Journal of Physics: Conference Series*, volume 100, page 062028. IOP Publishing.

Seyyedhabashy, M. M., Tafreshi, M. A., Shafiei, S., et al. (2020). Damage studies on irradiated tungsten by helium ions in a plasma focus device. *Nuclear Engineering and Technology*, 52(4):827–834.

Shahbazi rad, Z., Shahriari, M., and Abbasi Davani, F. (2011). Investigation of Spatial Distribution of Hydrogen and Argon Ions and Effects of them on Aluminum Samples in a 2.5 kJ Mater Type Plasma Focus Device. *Journal of Fusion Energy*, 30(5):358–366.

Shirani, B. and Abbasi, F. (2010). Construction and experimental study of a 2.5 kJ, simply configured, Mather type plasma focus device. *Brazilian Journal of Physics*, 40:125–130.

Shirokova, V., Laas, T., Ainsaar, A., et al. (2013). Comparison of damages in tungsten and tungsten doped with lanthanum-oxide exposed to dense deuterium plasma shots. *Journal of Nuclear Materials*, 435(1-3):181–188.

Shirokova, V., Laas, T., Ainsaar, A., et al. (2014). Armor materials behavior under repetitive dense plasma shots. *Physica Scripta*, 2014(T161):014045.

Tesmer, J. R. and Nastasi, M. (1995). Handbook of modern ion beam materials analysis. *Materials Research Society, 9800 McKnight Rd, Suite 327, Pittsburgh, PA 15237, USA, 1995. 700*.

Väli, B., Laas, T., Paju, J., et al. (2016). The experimental and theoretical investigations of damage development and distribution in double-forged tungsten under plasma irradiation-initiated extreme heat loads. *Nukleonika*, 61(2):169–177.

Vas, J. V., Pan, J., Wang, N., et al. (2021). Plasma processed tungsten for fusion reactor first-wall material. *Journal of Materials Science*, 56(17):10494–10509.